BIOCHEMISTRY
including biophysical chemistry & molecular biology

Article

pubs.acs.org/biochemistry

Structure and Dynamics of the Acidosis-Resistant A162H Mutant of the Switch Region of Troponin I Bound to the Regulatory Domain of Troponin C

Sandra E. Pineda-Sanabria,[†] Ian M. Robertson,[‡] and Brian D. Sykes*[,†]

[†]Department of Biochemistry, [‡]Department of Pediatrics, Faculty of Medicine & Dentistry, University of Alberta, Edmonton, AB T6G 2H7, Canada

Supporting Information

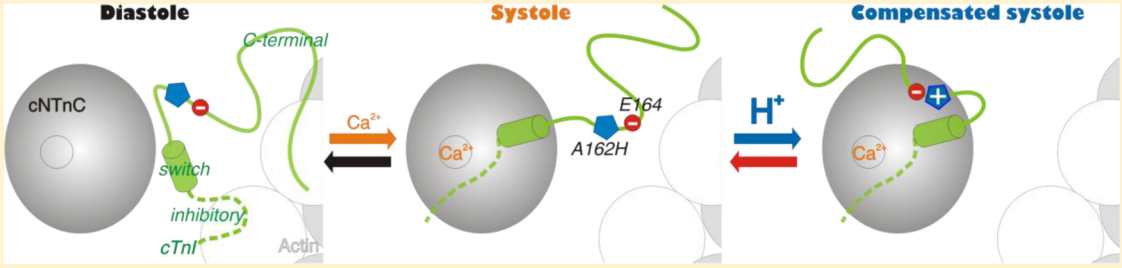

ABSTRACT: Intracellular acidosis lowers the Ca^{2+} sensitivity of cardiac muscle, which results in decreased force generation, decreased cardiac output, and, eventually, heart failure. The A162H mutant of cardiac troponin I in the thin filament turns the heart acidosis-resistant. Physiological and structural studies have provided insights into the mechanism of protection by the A162H substitution; however, the effect of other native residues of cardiac troponin I is not fully understood. In this study, we determined the structure of the A162H mutant of the switch region of cardiac troponin I bound to the regulatory domain of troponin C at pH 6.1, and the dynamics as a function of pH, by NMR spectroscopy to evaluate the changes induced by protonation of A162H. The results indicate that A162H induces a transitory curved conformation on troponin I that promotes contraction, but it is countered by residue E164 to ensure proper relaxation. Our model explains the absence of diastolic impairment in the gain-of-function phenotype induced by the A162H substitution as well as the effects of a variety of mutants studied previously. The description of this mechanism underlines the fine quality of regulation on cardiac muscle contraction and anticipates pharmacological agents that induce modest changes in the contraction−relaxation equilibrium to produce marked effects in cardiac performance.

In contrast to skeletal muscle, acidosis in the heart significantly diminishes the force of contraction of cardiac muscle and the overall capacity of the heart to pump blood. It has been shown that the change of a single residue from histidine (H130) in the skeletal isoform of troponin I (sTnI) to alanine (A162) in the cardiac isoform of troponin I (cTnI) is responsible for the observed differential sensitivity to acidosis.[1−3] Introducing the histidine into cTnI by mutagenesis in *in vitro* assays,[1] by gene transfer into failing human cardiomyocytes *ex vivo*,[2] or using transgenic mice *in vivo*[3] reverts the phenotype to that of skeletal muscle, conferring resistance to acidosis.

TnI is part of the heterotrimeric troponin (Tn) complex that regulates muscle contraction in response to intracellular Ca^{2+}. The Tn complex in cardiac and skeletal muscle is composed of TnT, TnI, and TnC subunits that orchestrate muscle contraction in response to Ca^{2+}. TnT is a long helical protein that interacts with TnI, tropomyosin, and actin to anchor the complex onto the thin filament. TnC contains two globular domains with two EF-hand motifs in each domain; the C-domain binds two Ca^{2+} or Mg^{2+} ions with high affinity and low specificity and interacts with TnI; the regulatory N-domain (NTnC) binds one Ca^{2+} ion with low affinity and high specificity and interacts with TnI only in the presence of Ca^{2+}. TnI is a long multihelical protein that interacts with TnT as well as both domains of TnC, and it inhibits contraction through its interaction with actin. When Ca^{2+} binds to NTnC, the switch region of TnI (switch-TnI) associates with NTnC, stabilizing the "open" conformation of NTnC, and drags the inhibitory region of cTnI off actin, resulting in movement of tropomyosin, exposure of the myosin binding sites on actin, and contraction.[4,5] This detailed description of the muscle architecture and the mechanism of contraction have been enabled largely by structural studies.

On the basis of the structures of skeletal and cardiac NTnC (sNTnC and cNTnC) bound to their respective switch regions of TnI (switch-sTnI and switch-cTnI), it was proposed that the introduction of A162H in the cardiac isoform induces

Received: February 21, 2015
Revised: April 17, 2015
Published: May 21, 2015

ACS Publications © 2015 American Chemical Society

DOI: 10.1021/acs.biochem.5b00178
Biochemistry 2015, 54, 3583−3593

electrostatic interactions with glutamate residues in cNTnC. The X-ray structure of the core skeletal complex[6] (1YTZ) shows the switch region of sTnI bound to sNTnC via a helix that interacts with the hydrophobic core of sNTnC followed by a curved region that contains H130 and interacts with helix A, possibly involving electrostatics with E20 of sNTnC. For the cardiac isoform, there are three structures that show switch-cTnI bound to cNTnC in the presence of Ca^{2+} (1MXL, 1J1E)[7,8] which all show that switch-cTnI forms a helix that interacts with the hydrophobic core of cNTnC just like in the skeletal isoform. The NMR structure (1MXL) and one molecule of the asymmetric unit from the X-ray structure (1J1E) show the region immediately following switch-cTnI in a random coil configuration that contains A162 and does not interact with cNTnC; in contrast, this region in the other molecule in the asymmetric unit forms a bent helix that extends to the C-terminus of switch-cTnI and does not interact with cNTnC. Zhou and collaborators showed that this region remains unstructured in solution using fluorescence anisotropy,[9] suggesting that the bent helix is probably an artifact of crystallization.[8] Investigation of acid dissociation constants (pK_a) on glutamate residues on cNTnC when bound to switch-sTnI, switch-cTnI, and switch-$cTnI_{A162H}$ confirmed electrostatic interactions between switch-sTnI and switch-$cTnI_{A162H}$, but not switch-cTnI, with E19 on cNTnC through H130 and H162, respectively.[10,11]

The mechanism of resistance to acidosis conferred by the A162H substitution has also been studied from a structural perspective. We recently published the structure of switch-sTnI bound to cNTnC at pH 6.[12] As predicted, the structure shows sTnI in the same conformation as sTnI when bound to sNTnC, with H130 in close proximity to E19. Because binding of the C-terminal region of cTnI to actin is necessary to achieve full inhibition, based on this structure and the orientation of sTnC in muscle fibers,[13] we proposed that introducing A162H in switch-cTnI increases Ca^{2+} sensitivity by increasing the affinity of switch-$cTnI_{A162H}$ for cNTnC via the additional H162−E19 interaction. This stabilizes the open conformation of cNTnC[11] and changes the orientation of the C-terminal region of cTnI away from actin,[12] the cNTnC and cTnI states that favor contraction. However, the structural studies using switch-sTnI do not take into account other residues besides H130 that differ in switch-cTnI, some of which have been suggested to have a role in the mechanism of resistance to acidosis,[14] and their impact on the structure of the switch-$cTnI_{A162H}$ mutant remains unclear.

In this work, we have determined the structure of switch-$cTnI_{A162H}$ bound to cNTnC at pH 6 by NMR. The structure addresses the structural changes induced by A162H in the presence of the other native switch-cTnI residues. The results indicate that protonation of H162 induces only a small positive potential in the pH-sensitive region due to the countering effect of native cardiac E164. This change, however, is sufficient to transiently change the conformation of switch-cTnI to one similar, but not identical, to that of switch-sTnI and to stabilize its interaction with cNTnC. We also evaluated the change in dynamics of the pH-sensitive region of $cTnI_{A162H}$ upon protonation of H162 to distinguish motion from structural heterogeneity. Our work explains the effect of a variety of previously studied TnI mutants along with the physiological effects of the A162H substitution on improving cardiac performance on the face of acidosis without causing diastolic dysfunction.

EXPERIMENTAL PROCEDURES

Materials and Sample Conditions. For structure determination, the recombinant human proteins ^{15}N-cNTnC and ^{15}N,^{13}C-cNTnC (residues 1−89) were expressed in *Escherichia coli* and purified as previously described,[15] and the synthetic peptide $cTnI_{A162H}$ (residues 144−170) containing the A162H substitution was obtained from GL Biochem Ltd. (Shanghai, China). To study backbone dynamics upon protonation of H162, we used a stable hybrid system that represents the cNTnC·switch-cTnI interaction during systole (cChimera)[16] to introduce the A162H substitution by site-directed mutagenesis of the original cChimera plasmid using the protocol described by Zheng.[17] The incorporation of the A162H substitution was confirmed by DNA sequencing, mass spectrometry, and NMR spectroscopy.

In the NMR experiments, all samples consisted of 500−600 μL of 100 mM KCl, 10 mM imidazole or imidazole-d_4, 10 mM $CaCl_2$, 10 mM dithiothreitol (DTT), and 0.25 mM 2,2-dimethyl-2-silapentane-5-sulfonate-d_6 sodium salt (DSS-d_6) as an internal standard. For structure determination, the sample contained 0.8−1 mM ^{15}N-cNTnC or ^{15}N,^{13}C-cNTnC and a 4:1 molar excess of $cTnI_{A162H}$ to ensure saturation of cNTnC, and the pH was set to 6.1. For backbone dynamics experiments, the sample contained 0.8 mM ^{15}N-$cChimera_{A162H}$ and the pH was set to 6.4 or 7.4 accordingly. For the pH titration of $cChimera_{A162H}$, the sample contained 0.7 mM ^{15}N-$cChimera_{A162H}$ and 2 mM piperazine to accurately determine pH values below 6.[18]

NMR Spectroscopy. All NMR experiments were acquired with Varian spectrometers of 500, 600, or 800 MHz at 30 °C. One-dimensional spectra were processed with VnmrJ, v.3.2 (Varian, Inc.), and multidimensional spectra were processed with NMRPipe[19] and analyzed with NmrViewJ.[20] Spectral assignments for the cNTnC·$cTnI_{A162H}$ complex were obtained by acquiring two- and three-dimensional experiments, as detailed in Supporting Information Table S1. Note that two independent ^{13}C,^{15}N -filtered NOESY NMR spectra were acquired, one at pH 6.1 and the other at pH 7.4, for assessment of conformational changes (* in Supporting Information Table S1). Assignments for $cChimera_{A162H}$ were guided by the assignment of wild-type cChimera,[16] homonuclear assignment of the $cTnI_{A162H}$ peptide (residues 144−173) bound to cNTnC, and the titration of unlabeled cNTnC into ^{15}N-$cTnI_{A162H}$ (Supporting Information Figure S1). All ^{15}N relaxation experiments were done at 600 MHz and acquired in random order with variable relaxation delays of 10, 100, 200, 500, 750, and 1000 ms for T_1 and 10, 30, 50, 70, 90, 110, and 150 ms for T_2. The data was fit to a two-parameter exponential decay curve using the Rate Analysis module of NMRViewJ, with the noise level used as an estimation of the standard deviation of the signal intensities.

Structure Determination. All experiments used to obtain distance restrains are detailed in Supporting Information Table S1. Intramolecular NOEs for cNTnC were calibrated in NMRViewJ with the median method. Intramolecular NOEs for $cTnI_{A162H}$ and intermolecular NOEs between cNTnC and $cTnI_{A162H}$ were classified as weak (1.8−6.0 Å). Intermolecular NOEs between cNTnC and Ca^{2+} were derived from crystallographic data. Dihedral angle restraints for cNTnC were determined using the TALOS+ server[21] (available at http://spin.niddk.nih.gov/bax/nmrserver/talos/) based on the chemical shifts of backbone atoms. For $cTnI_{A162H}$, −60 ± 25° and

DOI: 10.1021/acs.biochem.5b00178
Biochemistry 2015, 54, 3583−3593

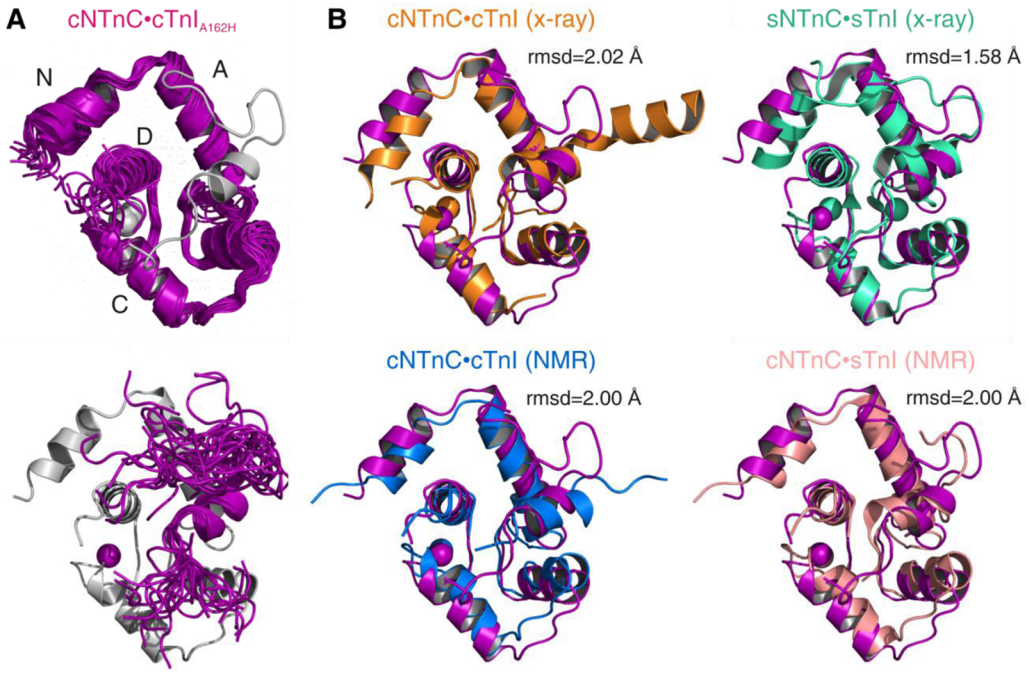

Figure 1. Structure of cNTnC·cTnI$_{A162H}$ compared with homologous complexes. (A) The ensemble of 20 structures is shown independently for cNTnC (top) and cTnI$_{A162H}$ (bottom) for clarity. The helices of cNTnC are labeled N and A–D. (B) Alignment and corresponding rmsd values for alpha carbons for all residues (1–89 and 144–170) for the present structure of cNTnC·cTnI$_{A162H}$ (purple) and the X-ray structures of cNTnC·cTnI (orange) and sNTnC·sTnI (green) as well as the NMR structures of cNTnC·cTnI (blue) and cNTnC·sTnI (pink). The Ca^{2+} atoms are displayed as spheres.

$-30 \pm 25°$ were used for φ and ψ dihedral angles, respectively, for residues for which the chemical shift index and random coil index indicated helical values according to their backbone ^{1}H chemical shifts. The distance and dihedrals experimental constraints were used in the simulated annealing module of Xplor-NIH, version 2.35.[22] To improve the quality of backbone and side chain conformations, we used the statistical torsion angle potential[23] of Xplor-NIH based on a database of over a million residues from high-quality crystal structures; we also used the gyration volume potential term to restrain the volume associated with the gyration tensor also based on values observed in the Protein Data Bank (PDB). Initially, 100 structures were calculated, from which the lowest-energy structure was used as the starting point for refinement. The final ensemble consisted of the 20 lowest-energy structures from the refinement step with no NOE or dihedral violations greater than 0.5 Å and 5°, respectively, and was validated with Procheck using the Protein Structure Validation Suite (PSVS 1.5) server available at http://psvs-1_5-dev.nesg.org/.

RESULTS

Structure of cNTnC·cTnI$_{A162H}$. The overall conformation of the cNTnC·cTnI$_{A162H}$ complex has structural elements of the cardiac and skeletal wild-type complexes (Figure 1A). The number and type of restraints used in the structure determination are shown in Supporting Information Table S2 along with scores from the structure validation. The structure coordinates have been deposited in the PDB under the ID 2MZP, and the NMR data for this system, in the BMRB under the ID 25495. The root-mean-square deviation (rmsd) of alpha carbons for all residues with the X-ray structure of the cardiac (1J1E) and skeletal (1YTZ) Tn complexes is 2.02 and 1.58 Å, respectively; for helical components, the rmsd values are 1.70 and 1.19 Å, indicating higher similarity with the structure of the skeletal isoform of the complex (Figure 1B), mostly due to the differences in the C-terminus of the cTnI$_{A162H}$ peptide.

Structure of cNTnC in the cNTnC·cTnI$_{A162H}$ Complex. The conformation of cNTnC when bound to cTnI$_{A162H}$ is not significantly changed by the A162H substitution. Three-dimensional NOESY-NHSQC and NOESY-CHSQC NMR spectra were used to obtain the intramolecular distance information for cNTnC. A total of 1108 NOE and 157 dihedral restraints were used in the annealing and refinement protocols of Xplor-NIH[22] for this subunit of the complex. The structure displays five α-helices, N and A–D, of which the A–D helices are well-defined and the N-helix is more variable among models. There is also a short antiparallel β-sheet like in all other cTnI-bound structures of cNTnC. Comparing NTnC domains only, the rmsd of alpha carbons with the X-ray cardiac structure (1J1E) is 1.60 Å for all residues and 1.46 Å for residues in helical regions; compared to the X-ray skeletal structure (1YTZ), the rmsd for all residues is 1.58 Å, and for residues in helical regions, 1.19 Å.

Structure of cTnI$_{A162H}$ in the cNTnC·cTnI$_{A162H}$ Complex. The experimental data localizes cTnI$_{A162H}$ on the hydrophobic patch of cNTnC and dictates a curved conformation similar to that of sTnI. The two-dimensional $^{13}C,^{15}N$-filtered NOESY NMR spectrum was used to obtain the intramolecular distance restraints for the cTnI$_{A162H}$ peptide (Figure 2), whereas the three-dimensional edited ^{13}C-filtered NOESY-CHMQC NMR spectrum provided the intermolecular distance restraints for the cNTnC·cTnI$_{A162H}$ interaction (Figure 3). A total of 140 intramolecular and 34 intermolecular NOEs and 13 dihedral restraints were used in the structure determination. The intramolecular NOEs between H162 and residues M154 and Q155 on the switch helix are consistent

DOI: 10.1021/acs.biochem.5b00178
Biochemistry 2015, 54, 3583–3593

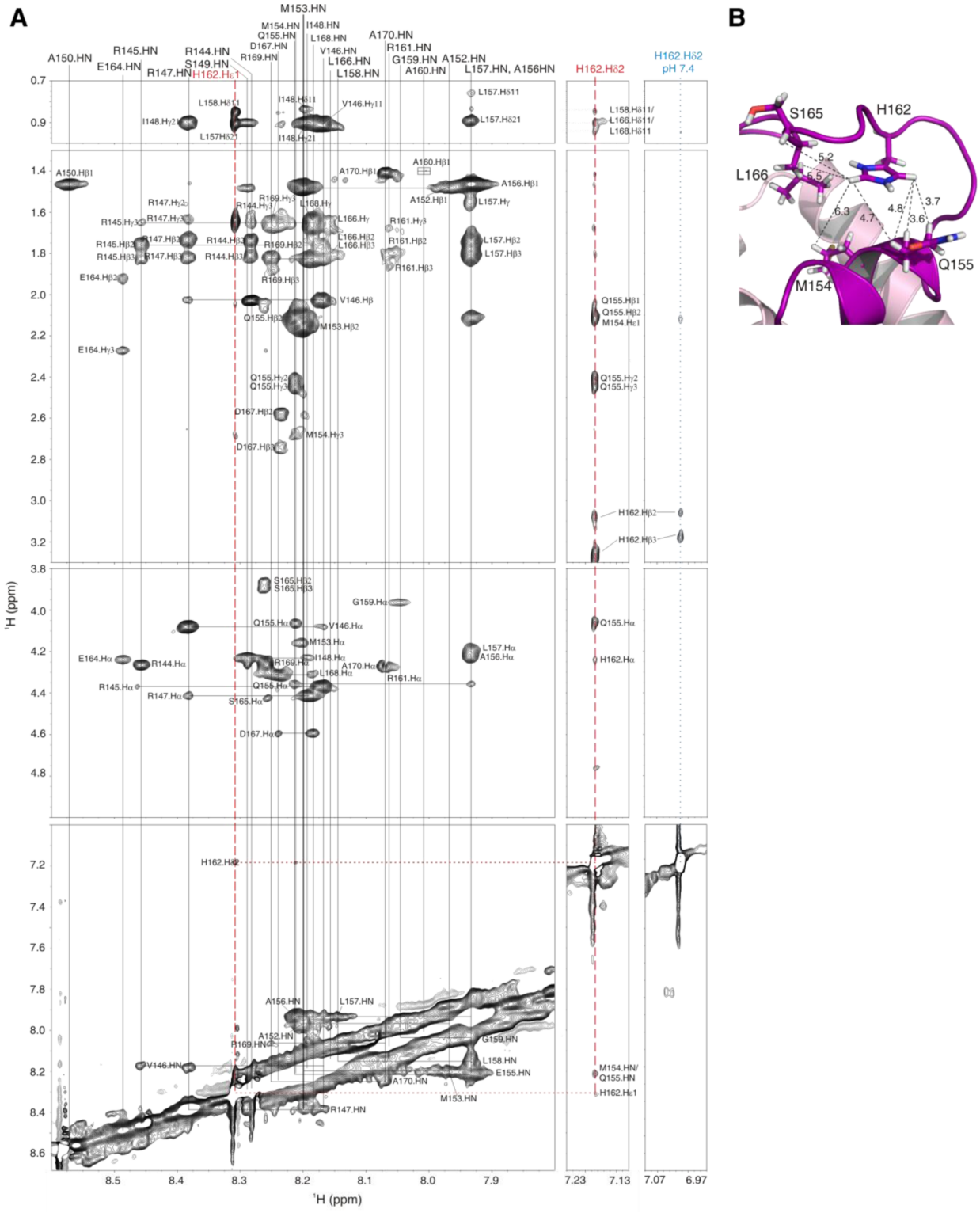

Figure 2. Intramolecular NOEs for $cTnI_{A162H}$. (A) Strip plots of the $^{13}C,^{15}N$-filtered noesy NMR spectrum showing the intramolecular contacts used in the structure calculation at pH 6.1. The resonances of the $\delta 2$ and $\varepsilon 1$ protons of H162 are indicated by the red dashed lines. Ambiguous assignments are separated by a slash. The strip on the far right corresponds to the $\delta 2$ proton of H162 at pH 7.4 (blue dotted line). (B) Schematic of the contacts made by H162 within $cTnI_{A162H}$. Interatomic distances represented by dashed lines are in angstroms.

with the curved conformation of the switch peptide. When the pH was raised to 7.4 (blue dotted line in Figure 2A), only strong intraresidue NOEs are observed for the $\delta 2$ proton of H162; the lack of additional inter-residue contacts indicates an extended conformation for this region at physiological pH when H162 is not protonated. The intermolecular NOEs position $cTnI_{A162H}$ between helices A, B, and D of cNTnC. Residues V146 and I148 on the N-terminal region of $cTnI_{A162H}$ contact M60 on the C-helix and L48 and Q50 on helix B of cNTnC, respectively, localizing this region toward helix C. The

DOI: 10.1021/acs.biochem.5b00178
Biochemistry 2015, 54, 3583−3593

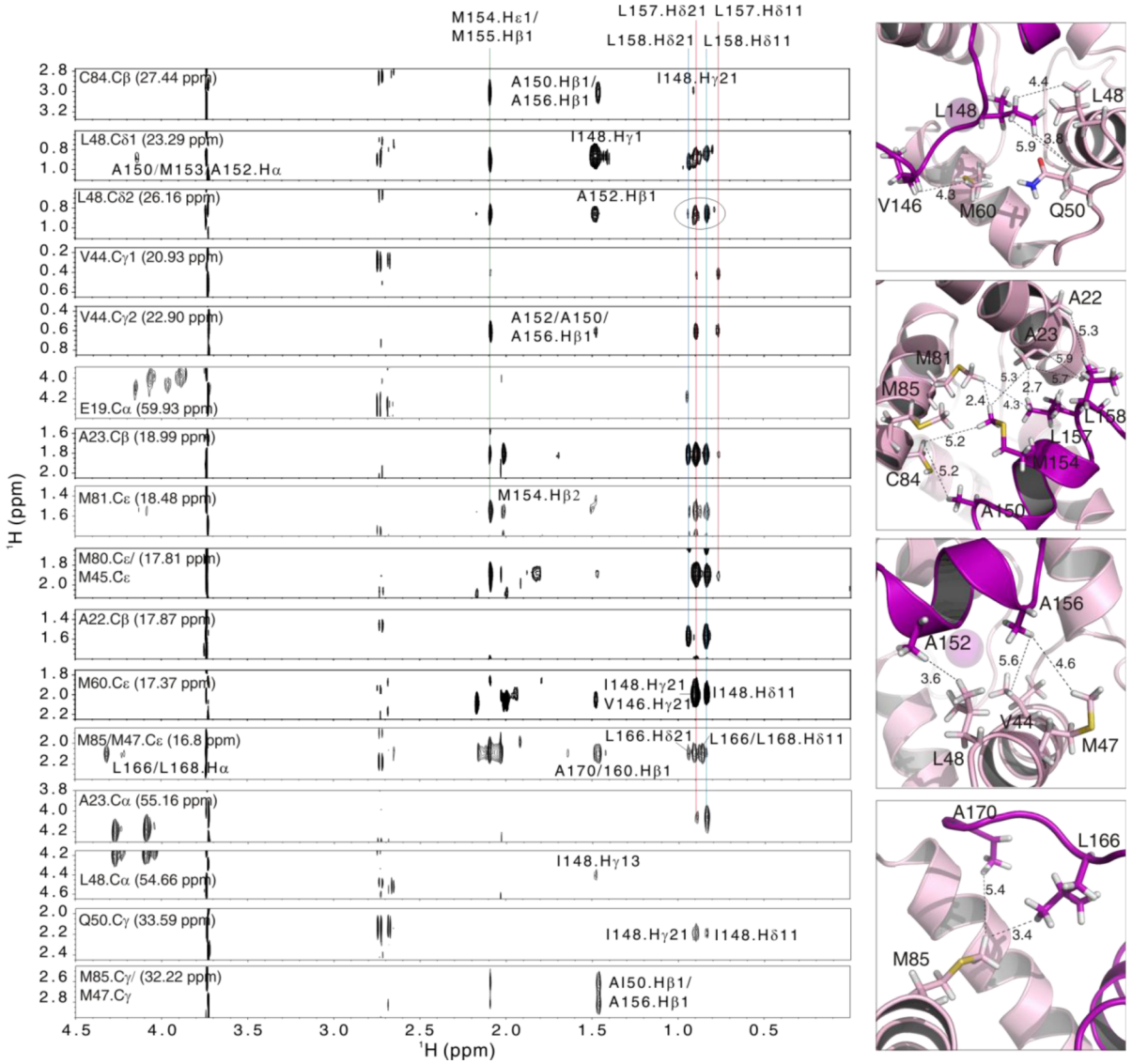

Figure 3. Intermolecular NOEs for cNTnC·cTnI$_{A162H}$. Strip plots from the ^{13}C-filtered NOESY-CHMQC NMR spectrum showing the intermolecular NOEs used in the structure calculation. The schematics on the right illustrate from top to bottom contacts involving the N-terminal, helical, and posthelical regions of cTnI$_{A162H}$. Dashed lines indicate interatomic distances in angstroms.

NOEs from the switch helix can be divided into two groups, one group formed by A150, M154, L157, and L158 defines one side of the helix and contacts residues A22 and A23 on helix A of cNTnC and M81, C84, and M85 on helix D. The other group, formed by residues A152 and A156, lies on the opposite side of the helix and contacts residues V44, M47, and L48 on the B helix of cNTnC, positioning the switch helix in the hydrophobic groove of cNTnC. Following the helical region, residues L166 and A170 contact residue M85 on helix D of cNTnC, thereby restricting the C-terminal side of the cTnI$_{A162H}$ peptide and contributing to its curved conformation. The pH-sensitive region (residues 161−164) is less constrained than the switch helix, with the distance from protons δ2 and ε1 of H162 to β of E19 varying from 8.2 to 14.7 Å and to the γ protons from 8.5 to 16.2 Å within the final ensemble.

Comparing the TnI segments only with the cardiac (1J1E) and X-ray skeletal (1YTZ) structures, the respective rmsd values based on alpha carbons are 12.98 and 3.70 Å for all residues, 0.19 and 0.25 Å for residues on the switch helix only (150−157), and 17.95 and 4.08 Å for residues after the switch helix (158−170), indicating higher resemblance to sTnI; however, and despite the closer sequence similarity with sTnI introduced by H162 (Figure 4A), a consistent difference in the pH-sensitive region is observed. In all models, H162 on the pH-sensitive region lies farther away from helix A compared to sTnI, and in the model where H162 is in a similar position to H130 of sTnI, helix A and E19 are pushed away (Figure 4B,C). To investigate if these differences are genuine or are a consequence of structural heterogeneity, we studied the backbone dynamics of the pH-sensitive region in different protonation states of H162.

Protonation of H162. For the measurement of the dynamics of the pH-sensitive region of TnI$_{A162H}$ as a function of the protonation state of H162, we used a cTnC−cTnI chimera containing the A162H substitution (cChimera$_{A162H}$) based on the wild-type cChimera, which reliably represents the cNTnC·switch-cTnI complex but offers superior stability, solubility, and 1:1 stoichiometry.[16] cChimera consists of cNTnC attached to cTnI (residues 144−173) by a flexible cleavable linker; it preserves the structural features of the

DOI: 10.1021/acs.biochem.5b00178
Biochemistry 2015, 54, 3583−3593

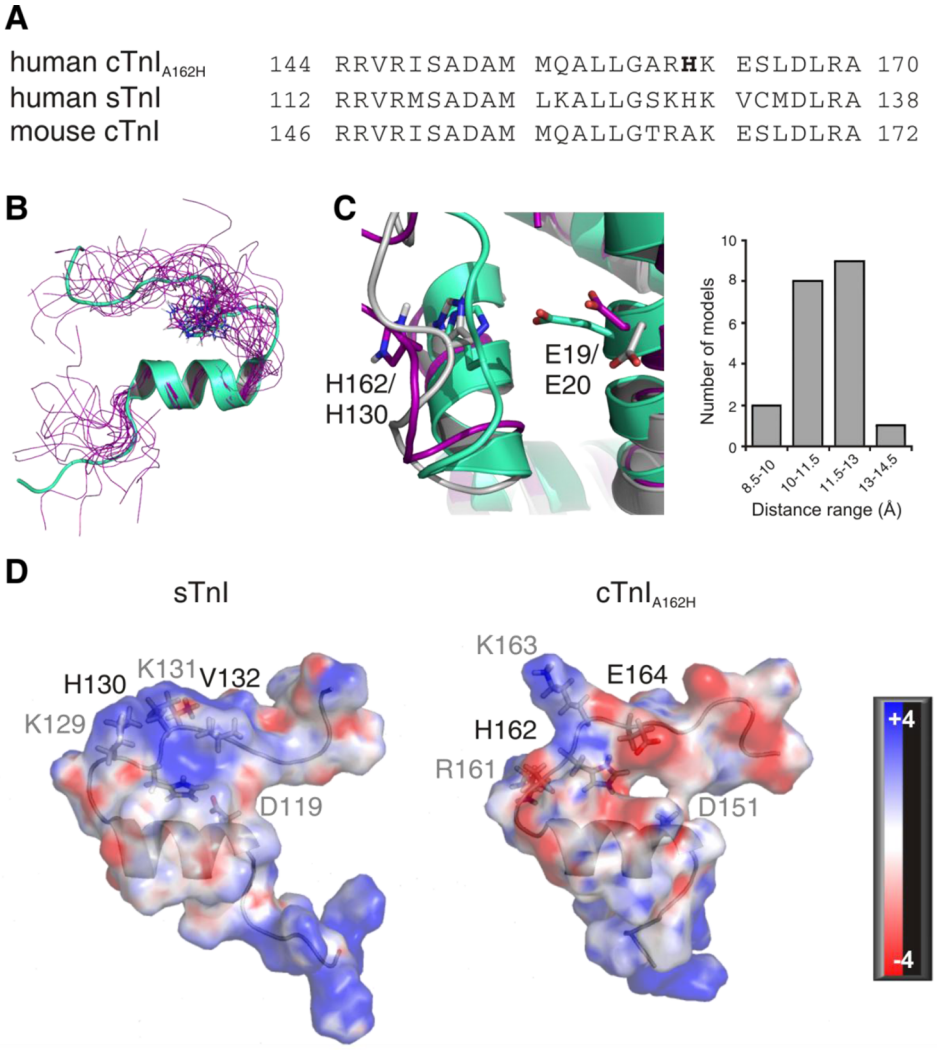

Figure 4. Comparisons of cTnI$_{A162H}$ and sTnI. (A) Sequence alignment of cTnI$_{A162H}$ with the homologous regions of sTnI and mouse cTnI for reference; the site of mutation is in bold. (B) The structure alignment of the switch helix of cTnI$_{A162H}$ (purple, residues 150−157) and sTnI (green, residues 118−125) from the X-ray structure (1YTZ) shows similar peptide conformation. (C) An expansion of the pH-sensitive region shows variable location of H162 of cTnI$_{A162H}$ (purple and gray) compared to sTnI. The histogram displays the distribution of average distances between the $\delta 2/\varepsilon 1$ protons of H162 and the β/γ protons of E19 within the 20 lowest-energy structures. (D) Electrostatic potential mapped on the surface of sTnI and cTnI$_{A162H}$; residues labeled in black are on the side of TnI that faces cNTnC, whereas those in gray are on the other side that faces the solvent.

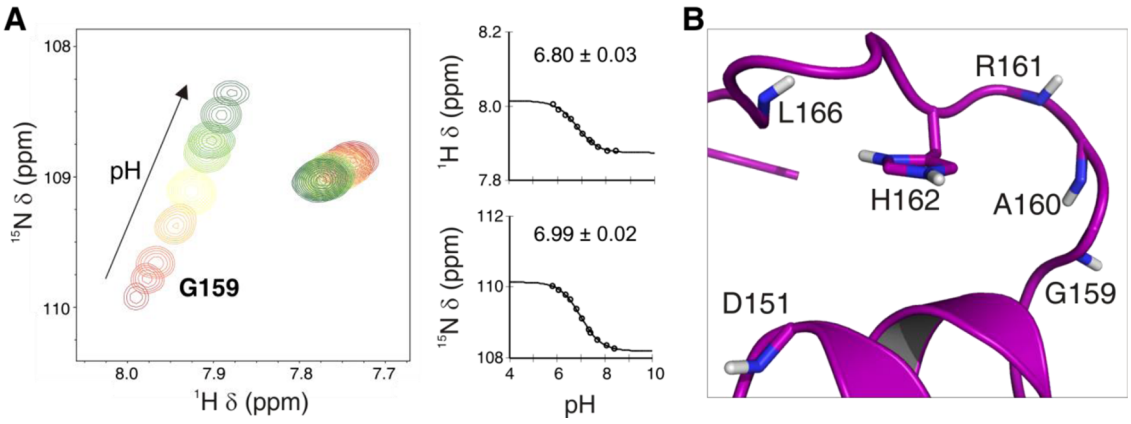

Figure 5. Determination of pK_a for H162 in cChimera$_{A162H}$. (A) Overlap of a section of the ^{1}H,^{15}N correlation spectra of cChimera$_{A162H}$ for the pH range from 5.81 to 8.40 (red to green), curve fitting, and pK_a^{app} for residue G159. The error indicates the standard deviation of the fit. (B) Location of residue G159 relative to H162 in the present structure.

DOI: 10.1021/acs.biochem.5b00178
Biochemistry 2015, 54, 3583−3593

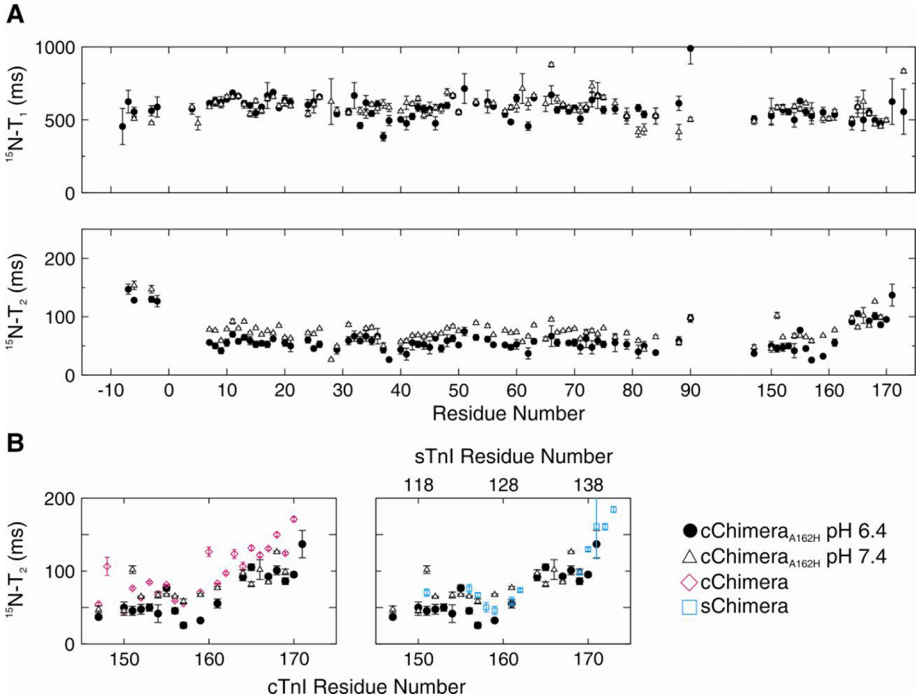

Figure 6. Dynamics of cChimera$_{A162H}$. (A) ^{15}N-T$_1$ and ^{15}N-T$_2$ relaxation times for the backbone NH pairs of cChimera$_{A162H}$ when H162 is protonated (filled circles) and deprotonated (empty triangles). (B) Comparison of ^{15}N-T$_2$ profiles for the TnI region of protonated and deprotonated cChimera$_{A162H}$ with cChimera (left) and sChimera (right).

Table 1. T$_1$ and T$_2$ Values for Various Regions of cChimera$_{Al62H}$

	T$_1$ (ms ± SE)		T$_2$ (ms ± SE)	
cChimera$_{A162H}$ region (residues)	pH 7.4	pH 6.4	pH 7.4	pH6.4
full cChimera$_{A162H}$	588 ± 26	579 ± 39	78 ± 3	65 ± 7
cNTnC (1−89)	597 ± 27	585 ± 31	72 ± 2	54 ± 7
cTnI$_{Al62H}$ helix (150−157)	580 ± 33	552 ± 37	61 ± 3	48 ± 6
cTnI$_{Al62H}$ C-terminus (158−170)	534 ± 23	522 ± 44	92 ± 4	82 ± 4
cTnI$_{A162H}$ pH-sensitive (157−163)	554 ± 29	538 ± 42	68 ± 2	38 ± 4

original cNTnC·cTnI$_{144-173}$ complex corresponding to the systolic state of the heart due to a high apparent concentration of switch-cTnI. Because this is a more soluble and stable system that allows us to directly observe the ^{1}H and ^{15}N resonances of residues in cTnI once it is bound to cNTnC, it is ideally suited for the focused investigation of the protonation of H162 and the dynamics of the pH-sensitive region of cTnI$_{A162H}$.

We performed a pH titration of cChimera$_{A162H}$ monitored by ^{1}H,^{15}N-HSQC NMR experiments at each titration point to investigate the pK_a of H162 in this system. The pK_a of a specific residue can be determined by plotting the chemical shift change as a function of the pH. In the pH titration, the backbone ^{1}H and ^{15}N amide resonances of titratable residues and some nontitratable residues of cChimera$_{A162H}$ were pH-sensitive, especially around the site of the mutation (Figure 5 and Supporting Information Figure S2). Although H162 displays a very weak signal located in a crowded region of the spectrum, making direct pK_a determination difficult and inaccurate, its pK_a could be determined indirectly by analyzing nearby residues for which a pK_a is not expected (nontitratable) but where an apparent pK_a (pK_a^{app}) was observed, as well as from residues for which the observed pK_a value is far from the expected, as previously done for other related complexes.[10,11] According to the conformation observed in our structure of cNTnC·cTnI$_{A162H}$, the residues closest to H162 that displayed large chemical shift changes are G159, A160, R161, and L166; in addition, D151 at the beginning of the switch helix was also analyzed to investigate intermolecular interactions within the cTnI$_{A162H}$ region. On the basis of their ^{1}H resonances, the pK_a of H162 in cChimera$_{A162H}$, expressed as the average ± standard deviation, is 6.82 ± 0.06; on the basis of their ^{15}N resonances, the value is 6.78 ± 0.06, yielding a combined average of 6.80 ± 0.06, the same as determined previously in the cNTnC·switch-cTnI$_{A162H}$ complex (6.82 ± 0.28).[11] Knowing the pK_a, we can determine the protonation state of H162 in cChimera$_{A162H}$ at different pH values in order to choose representative but physiological conditions. According to the Henderson−Hasselbalch equation, H162 is 20 and 72% protonated at pH 7.4 and 6.4, respectively, values that have physiological relevance and represent different protonation states of H162 for the dynamics analysis.

Dynamics of cTnI$_{A162H}$. To evaluate changes in the dynamics of cTnI$_{A162H}$ upon protonation of H162, we determined the T$_1$ and T$_2$ relaxation times for the backbone amide NH pairs of cChimera$_{A162H}$ at pH 7.4 and 6.4 (Figure 6A). The data has been deposited in the BMRB under the ID 25511. Average T$_1$ and T$_2$ values are listed in Table 1 for the different regions of cChimera$_{A162H}$. The T$_1$ profile was very similar at the two pH values tested. The T$_2$ profiles at the two pH values were very similar but consistently lower for the

DOI: 10.1021/acs.biochem.5b00178
Biochemistry 2015, 54, 3583−3593

cNTnC region due to a slight tendency to aggregation as the pH lowers closer to 6.[24] The T_2 data indicates that the most pH-sensitive region corresponds to cTnI residues 157 to prior to 164, which has the highest significant difference between the different pH values (Table 1). The $cTnI_{A162H}$ region also displays a plateau from residues 164−170 at both pH values.

DISCUSSION

Myocardial contraction is a vital process that requires fine regulation of the contraction−relaxation equilibrium to ensure the survival of the organism and the species. Several mechanisms control cardiac performance, but one of the most intrinsic levels of regulation is the sensitivity of cTnC for Ca^{2+}. Two modulators of Ca^{2+} sensitivity that favor relaxation have evolved in cardiac muscle: phosphorylation and pH-dependent sensitivity. Only the cardiac isoform of TnI contains an N-terminal extension that can be phosphorylated at residues S22 and S23 by PKA and disrupt interactions of the N-terminal extension with cNTnC, resulting in a decrease in Ca^{2+} sensitivity on the thin filament in response to adrenergic stimulation.[25−27] The other mechanism is the replacement of H130 in sTnI for A162 in the analogous position of cTnI, which, according to an evolutionary model,[28] lowered the Ca^{2+} sensitivity of the cardiac thin filament in higher-order chordates in response to less demanding environmental conditions compared to those of cold water fish and amphibians,[28] but it made the heart muscle vulnerable to low-pH conditions such as hypoxia and myocardial ischemia. Placing the histidine in cTnI, as the A162H mutant, produces a gain-of-function phenotype at pH ∼ 6, protecting the heart from intracellular acidosis.

In this study, we determined the structure and dynamics of the cNTnC·$cTnI_{A162H}$ complex to address the effect of the A162H substitution in the presence of other native cTnI residues. When comparing the present structure of cNTnC·$cTnI_{A162H}$ with homologous complexes, the NTnC subunit is unchanged overall and the differences are mostly in the TnI subunit (Figure 1B). The cTnI subunits of all of these complexes display the switch helix interacting with the hydrophobic patch of cNTnC; however, two different conformations can be distinguished for the pH-sensitive region (residues 161−164 for cardiac or residues 129−132 for skeletal). One conformation is extended with the pH-sensitive region pointing away from the switch helix and is observed in the X-ray and NMR structures of cNTnC·cTnI. The other conformation is curved with the pH-sensitive region parallel to the switch helix and is observed in the structures of sTnI bound to sNTnC or cNTnC as well as in the present structure as the result of electrostatic interactions between the positively charged H130/H162 of sTnI/$cTnI_{A162H}$ and E20 of sNTnC or E19 of cNTnC, as shown previously.[11,12] Importantly, the lack of intramolecular NOEs between H162 and other cTnI residues at pH 7.4 in our present study (Figure 2A) indicates that $cTnI_{A162H}$ adopts the extended conformation when bound to cNTnC at physiological pH. We previously proposed that the extended conformation favors relaxation in cardiac muscle by positioning the C-terminal region of cTnI, necessary for its full inhibitory activity, close to actin in the thin filament, whereas the curved conformation of sTnI positions the C-terminal region away from actin favoring contraction.[12]

The conformation observed for $cTnI_{A162H}$ in this study is curved, similar to that observed for sTnI when bound to either sNTnC or cNTnC, but the location of the pH-sensitive region is slightly different (Figure 4B,C). Previous data point to a curved conformation for $cTnI_{A162H}$, such as the demonstration of electrostatic interactions between H162 and E19 and E15 of cNTnC, the preservation of the curved conformation of sTnI when binding to cNTnC, and the great similarity of intramolecular NOE contacts for sTnI and $cTnI_{A162H}$ when bound to cNTnC.[11,12] While the intermolecular NOEs that dictate the localization of the peptides are very similar between sTnI and $cTnI_{A162H}$ when bound to cNTnC, the actual localization of their pH-sensitive regions is slightly different with H162 positioned further from cNTnC compared to H130.

One explanation for the different localization of $cTnI_{A162H}$ and sTnI is that the electrostatic potential of $cTnI_{A162H}$ on the pH-sensitive region is more negative and therefore may shift it farther from E19 of cNTnC compared to sTnI via electrostatic repulsion. We previously showed that the position of the pH-sensitive region of sTnI bound to sNTnC and cNTnC was the same,[12] which indicates that the difference observed in the present $cTnI_{A162H}$ structure results from other residues within the $cTnI_{A162H}$ peptide. From the residues neighboring H162/H130, the most significant difference in the sequence corresponds to E164 in $cTnI_{A162H}$ substituted for V132 in sTnI introducing an extra negative charge in $cTnI_{A162H}$. To investigate how E164 impacts peptide electrostatics, we used the Delphi web server[29,30] (available at http://compbio.clemson.edu/delphi_webserver/) to calculate the electrostatic potential of the $cTnI_{A162H}$, cTnI, and sTnI peptides using a linear solver for the Poisson−Boltzmann equation. Figure 4D shows the potential mapped onto each TnI peptide; although $cTnI_{A162H}$ and sTnI have three consecutive positively charged residues, in the structure two of them lie on the side of TnI that faces the solvent and only one (H162/H130) faces cNTnC along with V132 in sTnI, which is neutral, or E164 of $cTnI_{A162H}$, which displays a strong negative potential. Then, in sTnI, the mostly positive potential generated by H130 favors interactions with E19, whereas in $cTnI_{A162H}$, the negative potential prevents closer interactions. In fact, the average distance from the $\delta 2$ and $\varepsilon 1$ protons of H162 to the β protons of E19 is 11.2 Å and to the γ protons, is 12.0 Å, which constitutes a larger separation compared to 7.2 and 7.6 Å for H130−E19 and H130−E20, respectively.[12] Despite the repulsive effect of E164, the presence of the small positive potential of H162 is enough to produce a positive inotropic effect in the hearts and myocytes of transgenic mice expressing $cTnI_{A164H}$ (mouse numbering, Figure 4A) and in myocytes from failing human hearts transduced with $cTnI_{A164H}$,[2] which underlines the significance of electrostatics in the mechanism of contraction enhancement by the A162H substitution.

Stabilization and a conformational change of switch-$cTnI_{A162H}$ upon protonation of H162 are also supported by our backbone dynamics. The drop in T_2 observed for residues 157−160 (pH sensitive loop) immediately following the switch helix indicates increased rigidity or exchange broadening in that region upon protonation of H162. Increased rigidity can correlate with stabilization of the pH-sensitive loop in a curved conformation via the H162−E19 interaction; this also correlates with the increased affinity of switch-$cTnI_{A162H}$ for cNTnC at pH 6 observed previously.[11] Stabilization of the curved conformation could also be mediated by intramolecular interactions between H162 and D151 on the switch helix, as D151 displayed an average pK_a^{app} of 6.86 ± 0.08, corresponding to H162 of $cTnI_{A162H}$; however, its pK_a could not be determined due to precipitation of $cChimera_{A162H}$ under pH 5.5. Exchange broadening is an indication of different

DOI: 10.1021/acs.biochem.5b00178
Biochemistry 2015, 54, 3583−3593

conformations that interconvert with each other; in this case, protonation of H162 may induce transient interactions with E19 that cause the loop to change its conformation. Another feature of the T_2 profile under both pH conditions is the presence of a plateau, which indicates that residues 164−170 tumble together in solution as a single unit. The dynamics of protonated and deprotonated $cTnI_{A162H}$ approximate the dynamics of the homologous regions of sTnI and cTnI, respectively. The relaxation parameters of the TnI regions for skeletal and cardiac isoforms have been studied before using hybrid proteins. We compared the T_2 profiles at 600 MHz of the TnI region of $cChimera_{A162H}$ at pH 6.4 and 7.4 (this work) with the TnI regions of cChimera at pH 6.9[16] (Figure 6B, left) and of sChimera at pH 6.8[31] (Figure 6B, right). There is a large degree of overlap between $cChimera_{A162H}$ at pH 7.4 and cChimera up to residue 164, where the T_2 plateau starts; this indicates that in that region $cTnI_{A162H}$ resembles native cTnI when H162 is uncharged. On the other hand, although there are some data points missing for sChimera, $cChimera_{A162H}$ at pH 6.4 is closer to sChimera than to cChimera, indicating that the pH-sensitive region of $cTnI_{A162H}$ when H162 is protonated is similar, but not identical, to the corresponding region of sTnI.

We propose that in the thin filament small changes in charge complementarity between the pH-sensitive region of TnI and helix A of cNTnC dictate the inclination of the contraction−relaxation equilibrium. The effects of charge substitutions in TnI have been studied in the past using different mutants of sTnI and cTnI.[1,2,14,32] For example, the $sTnI_{V134E}$ ($sTnI_{V132E}$) mutant was shown to decrease Ca^{2+} sensitivity to cardiac levels in myocytes but only at pH 6.2.[14] [The numbering for the mouse protein used in the original publications is given in the text with the homologous human numbering in parentheses. The sequence of mouse cTnI is shown in Figure 4A. Only human protein numbering is used in Figure 7 for clarity.] However, the reverse mutant, $cTnI_{Q155R/E164V}$, did not show any increase in Ca^{2+} sensitivity in an actomyosin ATPase assay.[1] Also, the $cTnI_{Q155R/A162H/E164V}$ mutant displayed improved Ca^{2+} sensitivity at pH 6.5 in the ATPase assay.[1] This can be explained by our present findings. The presence of a positive residue at position 162/130 on the side facing cNTnC will enhance contraction by inducing a curved conformation of TnI and positioning the C-terminal region away from actin; however, the stability of the curved conformation will be dictated by the amount of positive potential on the side that faces cNTnC (Figure 7). At the same time, the pH and the charge of the neighboring residues on that side can alter the amount of positive potential. Thus, low intracellular pH will stabilize the curved conformation by increasing the fraction of protonated H162/130 and the positive potential. In addition, along with H162/130, the simultaneous presence of neutral residues like V132 has no effect, whereas acidic residues like E164 counteract the positive potential, producing only a transient curved conformation that stills enhances contraction but allows efficient conversion to the extended conformation that facilitates relaxation, as in the case of the $sTnI_{V134E}$ ($sTnI_{V132E}$) and $cTnI_{A164H}$ ($cTnI_{A162H}$) mutants, which do not cause diastolic failure.[14,33] According to this model, introducing basic residues at position 164/132 (cardiac/skeletal numbering) may further enhance contraction at the cost of impairing relaxation. On the other hand, in the absence of H162/130, the conformation of TnI in the pH-sensitive region is extended, keeping the C-terminal region of TnI close to actin to favor

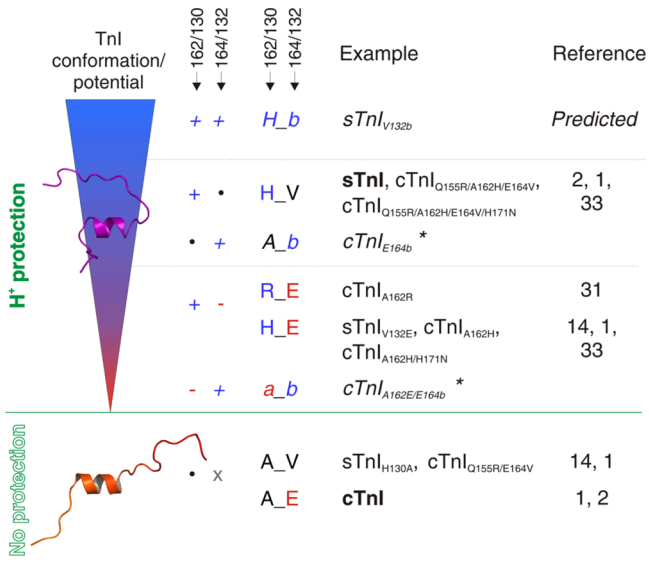

Figure 7. Model of H^+ protection. The stability of the curved conformation of the pH-sensitive region of cTnI that confers protection against acidosis depends on the amount of positive electrostatic potential of the side of cTnI that faces cNTnC, determined first by the residue type found at position 162/130 (cardiac/skeletal numbering) and then by the residue type present at position 164/132 in a gradual pH-dependent manner. The curved conformation and H^+ protection are lost once residue 162/130 becomes a noncharged residue. Different TnI mutants are localized in their corresponding levels on the electrostatic potential gradient, or in the no-protection zone, and the residues present at their 162/130 and 164/132 positions are specified. Native cTnI and sTnI are shown in bold. The + sign indicates a positively charged residue, −, a negatively charged residue, •, a hydrophobic residue, ×, a negatively or noncharged residue, a, an acidic residue, and b, a basic residue. Blue and red indicate positive and negative potentials, respectively. Predicted cases are in italics, and unknown cases are marked with an asterisk (*).

relaxation despite residue 164/132 being negative or neutral. This is the case for the $cTnI_{Q155R/E164V}$ mutant, which, despite containing the reverse $sTnI_{V134E}$ Ca^{2+}-desensitizing substitution, still shows the cardiac phenotype.[1] This model of "degrees of stabilization" also agrees with previous dynamics simulation data that show large structural variation for protonated $cTnI_{A164H}$ ($cTnI_{A162H}$) and more consistency for the constitutively charged $cTnI_{A164R}$ ($cTnI_{A162R}$) mutant on the formation of salt bridge with E19 of cNTnC.[32] Other mutants can also be explained by this model, such as the $sTnI_{H132A}$ ($sTnI_{H130A}$) mutant, which adopted the cardiac phenotype,[14] and the $cTnI_{A164R}$ ($cTnI_{A162R}$) mutant, which displayed enhanced contraction in transduced rat cardiomyocytes under acidic and baseline conditions due to a sustained positive charge at position 162.[32] The $cTnI_{Q157R/A164H/E166V/H173N}$ ($cTnI_{Q155R/A162H/E164V/H171N}$) and $cTnI_{A164H/H173N}$ ($cTnI_{A162H/H171N}$) mutants showed increased contractility in transduced rat cardiomyocytes under acidic conditions,[34] which fits our model, but also under baseline conditions despite the lack of a sustained positive charge at position 162, which suggests a role of residue N171 of sTnI (not studied yet independently) on enhancing contraction and is beyond the scope of our model. Finally, mutants that carry a positive charge at position 164/132 have not been reported and raise the question of the specificity of localization of the positive potential that induces the curved conformation (* in Figure 7).

DOI: 10.1021/acs.biochem.5b00178
Biochemistry 2015, 54, 3583−3593

Taken together, we conclude that the A162H substitution induces transient interactions of the partially positive pH-sensitive region with helix A of cNTnC to enhance contraction without impairing relaxation. The pK_a of the histidine residue and the consequent variability of its degrees of protonation make it optimal for maintaining muscle contraction in response to changing intracellular proton concentrations in the diseased heart. The understanding of this mechanism may aid in the pharmacological development of pH-sensitive agents that temporarily enhance the cTnI·cNTnC interaction to induce myocardial contraction without inducing diastolic dysfunction.

■ ASSOCIATED CONTENT

Supporting Information

Titration of cNTnC into ^{15}N-cTnI$_{A162H}$, full pH titration of cChimera$_{A162H}$, NMR experiments and parameters used, and statistics for the final ensemble of 20 structures. The Supporting Information is available free of charge on the ACS Publications website at DOI: 10.1021/acs.biochem.5b00178.

■ AUTHOR INFORMATION

Corresponding Author

*Phone: (+1) 780 492 3006. E-mail: brian.sykes@ualberta.ca.

Funding

This research project was funded by a CIHR grant (37769) to B.D.S., an AIHS studentship (3509) to S.E.P.-S., and a CIHR Fellowship (RES0020860) to I.M.R.

Notes

The authors declare no competing financial interest.

■ ACKNOWLEDGMENTS

The authors would like to thank David C. Corson for cNTnC purification and Peter C. Holmes and Jonathan Pan for assistance in HPLC purification of TnI peptides.

■ ABBREVIATIONS

cNTnC, the N domain of cardiac troponin C; cTnI, cardiac troponin I; cTnI$_{A162H}$, cardiac troponin I peptide from residues 144−170 containing the A162H substitution; DSS-d_6, 2,2-dimethyl-2-silapentane-5-sulfonate-d_6 sodium salt; DTT, dithiothreitol; NMR, nuclear magnetic resonance; NOE, nuclear Overhauser enhancement; NTnC, N-domain of troponin C; PDB, Protein Data Bank; pK_a, acid dissociation constant; pK_a^{app}, apparent pK_a; PSVS, protein structure validation suite; rmsd, root-mean-square deviation; sNTnC, the N domain of skeletal troponin C; switch-TnI, the switch region of troponin I; switch-cTnI, cardiac switch-TnI (residues 147−163); switch-cTnI$_{A162H}$, cardiac switch-TnI containing the A162H substitution; switch-sTnI, skeletal switch-TnI (residues 115−131); T_1, longitudinal relaxation time; T_2, transverse relaxation time; Tn, troponin; TnC, troponin C; TnI, troponin I; TnT, troponin T

■ REFERENCES

(1) Dargis, R., Pearlstone, J. R., Barrette-Ng, I., Edwards, H., and Smillie, L. B. (2002) Single mutation (A162H) in human cardiac troponin I corrects acid pH sensitivity of Ca^{2+}-regulated actomyosin S1 ATPase. *J. Biol. Chem. 277*, 34662−34665.

(2) Day, S. M., Westfall, M. V., Fomicheva, E. V., Hoyer, K., Yasuda, S., Cross, N. C. L., D'Alecy, L. G., Ingwall, J. S., and Metzger, J. M. (2006) Histidine button engineered into cardiac troponin I protects the ischemic and failing heart. *Nat. Med. 12*, 181−189.

(3) Palpant, N. J., Day, S. M., Herron, T. J., Converso, K. L., and Metzger, J. M. (2008) Single histidine-substituted cardiac troponin I confers protection from age-related systolic and diastolic dysfunction. *Cardiovasc. Res. 80*, 209−218.

(4) Kobayashi, T., Jin, L., and de Tombe, P. (2008) Cardiac thin filament regulation. *Pfluegers Arch. 457*, 37−46.

(5) Li, M., Wang, X., and Sykes, B. (2004) Structural based insights into the role of troponin in cardiac muscle pathophysiology. *J. Muscle Res. Cell Motil. 25*, 559−579.

(6) Vinogradova, M. V., Stone, D. B., Malanina, G. G., Karatzaferi, C., Cooke, R., Mendelson, R. A., and Fletterick, R. J. (2005) Ca^{2+}-regulated structural changes in troponin. *Proc. Natl. Acad. Sci. U.S.A.. 102*, 5038−5043.

(7) Li, M. X., Spyracopoulos, L., and Sykes, B. D. (1999) Binding of cardiac troponin-I147−163 induces a structural opening in human cardiac troponin-C. *Biochemistry 38*, 8289−8298.

(8) Takeda, S., Yamashita, A., Maeda, K., and Maeda, Y. (2003) Structure of the core domain of human cardiac troponin in the Ca^{2+}-saturated form. *Nature 424*, 35−41.

(9) Zhou, Z., Li, K., Rieck, D., Ouyang, Y., Chandra, M., and Dong, W. (2012) Structural dynamics of C-domain of cardiac troponin I protein in reconstituted thin filament. *J. Biol. Chem. 287*, 7661−7674.

(10) Robertson, I. M., Holmes, P. C., Li, M. X., Pineda-Sanabria, S. E., Baryshnikova, O. K., and Sykes, B. D. (2012) Elucidation of isoform-dependent pH sensitivity of troponin I by NMR spectroscopy. *J. Biol. Chem. 287*, 4996−5007.

(11) Pineda-Sanabria, S. E., Robertson, I. M., Li, M. X., and Sykes, B. D. (2013) Interaction between the regulatory domain of cardiac troponin C and the acidosis-resistant cardiac troponin I A162H. *Cardiovasc. Res. 97*, 481−489.

(12) Robertson, I. M., Pineda-Sanabria, S. E., Holmes, P. C., and Sykes, B. D. (2014) Conformation of the critical pH sensitive region of troponin depends upon a single residue in troponin I. *Arch. Biochem. Biophys. 552−553*, 40−49.

(13) Knowles, A. C., Irving, M., and Sun, Y. (2012) Conformation of the troponin core complex in the thin filaments of skeletal muscle during relaxation and active contraction. *J. Mol. Biol. 421*, 125−137.

(14) Westfall, M. V., and Metzger, J. M. (2007) Single amino acid substitutions define isoform-specific effects of troponin I on myofilament Ca^{2+} and pH sensitivity. *J. Mol. Cell. Cardiol. 43*, 107−118.

(15) Li, M., Saude, E., Wang, X., Pearlstone, J., Smillie, L., and Sykes, B. (2002) Kinetic studies of calcium and cardiac troponin I peptide binding to human cardiac troponin C using NMR spectroscopy. *Eur. Biophys. J. 31*, 245−256.

(16) Pineda-Sanabria, S., Julien, O., and Sykes, B. D. (2014) Versatile cardiac troponin chimera for muscle protein structural biology and drug discovery. *ACS Chem. Biol. 9*, 2121−2130.

(17) Zheng, L., Baumann, U., and Reymond, J. (2004) An efficient one-step site-directed and site-saturation mutagenesis protocol. *Nucleic Acids Res. 32*, e115−e115.

(18) Baryshnikova, O., Williams, T., and Sykes, B. (2008) Internal pH indicators for biomolecular NMR. *J. Biomol. NMR 41*, 5−7.

(19) Delaglio, F., Grzesiek, S., Vuister, G. W., Zhu, G., Pfeifer, J., and Bax, A. (1995) NMRPipe: A multidimensional spectral processing system based on UNIX pipes. *J. Biomol. NMR 6*, 277−293.

(20) Johnson, B. A., and Blevins, R. A. (1994) NMR view: a computer program for the visualization and analysis of NMR data. *J. Biomol. NMR 4*, 603−614.

(21) Shen, Y., Delaglio, F., Cornilescu, G., and Bax, A. (2009) TALOS+: A hybrid method for predicting protein backbone torsion angles from NMR chemical shifts. *J. Biomol. NMR 44*, 213−223.

(22) Schwieters, C. D., Kuszewski, J. J., and Marius Clore, G. (2006) Using Xplor-NIH for NMR molecular structure determination. *Prog. Nucl. Magn. Reson. Spectrosc. 48*, 47−62.

(23) Bermejo, G. A., Clore, G. M., and Schwieters, C. D. (2012) Smooth statistical torsion angle potential derived from a large conformational database via adaptive kernel density estimation

DOI: 10.1021/acs.biochem.5b00178
Biochemistry 2015, 54, 3583−3593

improves the quality of NMR protein structures. *Protein Sci. 21*, 1824−1836.
(24) Spyracopoulos, L., Gagné, S. M., Li, M. X., and Sykes, B. D. (1998) Dynamics and thermodynamics of the regulatory domain of human cardiac troponin C in the apo- and calcium-saturated states. *Biochemistry. 37*, 18032−18044.
(25) Robertson, S. P., Johnson, J. D., Holroyde, M. J., Kranias, E. G., Potter, J. D., and Solaro, R. J. (1982) The effect of troponin I phosphorylation on the Ca^{2+}-binding properties of the Ca^{2+}-regulatory site of bovine cardiac troponin. *J. Biol. Chem. 257*, 260−263.
(26) Solaro, R. J., Rosevear, P., and Kobayashi, T. (2008) The unique functions of cardiac troponin I in the control of cardiac muscle contraction and relaxation. *Biochem. Biophys. Res. Commun. 369*, 82−87.
(27) Hwang, P. M., Cai, F., Pineda-Sanabria, S. E., Corson, D. C., and Sykes, B. D. (2014) The cardiac-specific N-terminal region of troponin I positions the regulatory domain of troponin C. *Proc. Natl. Acad. Sci. U.S.A. 111*, 14412−14417.
(28) Palpant, N. J., Houang, E. M., Delport, W., Hastings, K. E. M., Onufriev, A. V., Sham, Y. Y., and Metzger, J. M. (2010) Pathogenic peptide deviations support a model of adaptive evolution of chordate cardiac performance by troponin mutations. *Physiol. Genomics 42*, 287−299.
(29) Smith, N., Witham, S., Sarkar, S., Zhang, J., Li, L., Li, C., and Alexov, E. (2012) DelPhi web server v2: Incorporating atomic-style geometrical figures into the computational protocol. *Bioinformatics 28*, 1655−1657.
(30) Sarkar, S., Witham, S., Zhang, J., Zhenirovskyy, M., Rocchia, W., and Alexov, E. (2012) DelPhi web server: a comprehensive online suite for electrostatic calculations of biological macromolecules and their complexes. *Commun. Comput. Phys. 13*, 269−284.
(31) Julien, O., Mercier, P., Allen, C. N., Fisette, O., Ramos, C. H. I., Lagüe, P., Blumenschein, T. M. A., and Sykes, B. D. (2011) Is there nascent structure in the intrinsically disordered region of troponin I? *Proteins. 79*, 1240−1250.
(32) Palpant, N. J., Houang, E. M., Sham, Y. Y., and Metzger, J. M. (2012) pH-responsive titratable inotropic performance of histidine-modified cardiac troponin I. *Biophys. J. 102*, 1570−1579.
(33) Palpant, N. J., D'Alecy, L. G., and Metzger, J. M. (2009) Single histidine button in cardiac troponin I sustains heart performance in response to severe hypercapnic respiratory acidosis in vivo. *FASEB J. 23*, 1529−1540.
(34) Thompson, B., Houang, E., Sham, Y., and Metzger, J. (2014) Molecular determinants of cardiac myocyte performance as conferred by isoform-specific TnI residues. *Biophys. J. 106*, 2105−2114.

DOI: 10.1021/acs.biochem.5b00178
Biochemistry 2015, 54, 3583−3593